Astron. Astrophys. 281, 864–870 (1994)

ASTRONOMY AND ASTROPHYSICS

Long-slit spectroscopy and direct imaging of the PMS objects GGD 33 and V 350 Cephei in NGC 7129

L.F. Miranda[1], C. Eiroa[2], M. Fernández[2], and A.I. Gómez de Castro[3]

[1] Departamento de Astrofísica, Facultad de Ciencias Físicas, Universidad Complutense de Madrid, E-28040 Madrid, Spain
[2] Departamento de Física Teórica, C-XI, Facultad de Ciencias, Universidad Autónoma de Madrid, Ciudad Universitaria de Canto Blanco, E-28049 Madrid, Spain
[3] ESA-IUE Observatorio, Villafranca Satellite Tracking Station, P.O. Box 50727, E-28080 Madrid, Spain

Received February 5, accepted June 13, 1993

Abstract. We present CCD images and long-slit spectra of the nebulous object GGD 33 and of the T Tauri star V 350 Cep in the star formation region NGC 7129. The data suggest that GGD 33a is a T Tauri star and likely the illuminating source of the whole GGD 33. Evidence of variability of GGD 33a is presented. Double-peaked [S II] emission lines are observed in GGD 33a. The high-velocity component of the [S II] emission could be related to a HH jet-like outflow observed very close to the star. V 350 Cep is embedded in a reflection nebulosity. High velocity mass outflow, detected through its blueshifted Hα emission, seems to emanate from V 350 Cep. The spectrum of V 350 Cep presents a large number of permitted emission lines, but, except [S II], no forbidden emission lines have been identified in our spectra.

Key words: stars: pre-main-sequence – stars: individual: V 350 Cep – ISM: individual objects: NGC 7129, GGD 33 (in NGC 7129) – ISM: jets and outflows

1. Introduction

Herbig–Haro (HH) objects are generated in the interaction between the energetic wind from a young star and the ambient cloud. However, the association of a particular young star with a particular HH object is not simple and in many cases it is unknown which star in a cloud is responsible for the excitation of a HH object. A good example in this respect is the star formation region NGC 7129, where a large number of HH objects is observed, including three collimated jets (Ray et al. 1990; Eiroa et al. 1992, hereafter EGM; Gómez de Castro et al. 1992; Miranda et al. 1993, hereafter MEG). Although extensive observations of NGC 7129 have been carried out (see Hartigan & Lada 1985 and EGM for a summary of the observations and references), exciting stars have definitively been identified only in the case of two of the jets (Ray et al. 1990; MEG). For several HH objects in NGC 7129 candidates to exciting stars have been suggested on the basis of morphological considerations or proper motions (Ray et al. 1990; EGM), but definitive spectroscopic confirmation is still lacking.

One of the dubious cases is the nebulous object GGD 33 (Gyuld'budagyan et al. 1978). Morphologically, GGD 33 consists of a compact region, GGD 33a, connected by a faint, curved nebulous arm to an extended nebulosity, GGD 33b. The observations show that the nebulous arm and GGD 33b are reflected light (EGM). On the other hand, the [S II] image by EGM shows a faint spike arising from GGD 33a embedded in the nebulous arm. This suggests that shock-excited material may also be present in the object. The nature of GGD 33a is controversial. Its spectrum shows strong H, [O I], [S II] and [Fe II] emissions (Cohen & Fuller 1985, hereafter CF; Goodrich 1986, hereafter GO), which led GO to suggest that GGD 33a is a peculiar HH object. GO proposed that the exciting star of GGD 33a and, hence, of GGD 33, is the variable T Tauri star V 350 Cep (Magakyan 1983; Cohen & Schwartz 1983; CF; GO), located $\approx 24''$ towards the northwest of GGD 33a. However, Magakyan (1983) and EGM pointed out the clear stellar appearance of GGD 33a and suggested that a young star could be embedded in the compact region.

In this paper we present direct images and long-slit spectra of GGD 33 and V 350 Cep. The data give new insights into the real nature of GGD 33a and also reveal new aspects of V 350 Cep.

2. Observations

2.1. Direct imaging

Direct images of GGD 33 and V 350 Cep were obtained in October 1990 at the prime focus of the 3.5 m telescope on the Calar Alto Observatory. A RCA CCD with

Send offprint requests to: L.F. Miranda

1024 × 656 pixels of 15 μm in size was used as detector. The scale on the focal plane is 0.254″ pixel^{-1} and the field of view 260″ × 162″. Two narrow-band filters were used: Hα ($\lambda_{ef} \approx 6580$ Å, FWHM ≈ 100 Å) and [S II] ($\lambda_{ef} \approx 6740$ Å, FWHM ≈ 70 Å). Exposure time was 1800 s in each case. The seeing was $\approx 1.1''$. The observations were bias-corrected and flat-fielded using standard procedures.

2.2. Long-slit spectroscopy

Long-slit spectra of GGD 33 and V 350 Cep were obtained in August 1989 with the Twin Cassegrain Spectrograph of the 3.5 m telescope. In the red channel of the spectrograph, the detector was a GEC CCD with 580 × 410 pixels of 17 μm in size. The spectral range 6470–6820 Å was covered at a dispersion of 36 Å mm^{-1}. In the blue channel, the detector was a RCA CCD with 1024 × 656 pixels of 15 μm in size. The spectral range 4235–5365 Å was covered at a dispersion of 72 Å mm^{-1}. The slit (240″ length) was centered on V 350 Cep and set to position angles (PAs) −90° and −55°, the later also covering GGD 33a and part of GGD 33b (see Fig. 1). Unfortunately, the [S II] spike was not covered by the slit. Exposure times were 1800 s (PA −90°) and 3600 s (PA −55°). A Fe–Ne lamp was used for wavelength calibration. Using a slit width of 2″, the achieved spectral resolution (FWHM) is ≈ 65 km s^{-1} in the red channel and ≈ 135 km s^{-1} in the blue channel. The spatial resolution (FWHM), mainly determined by the seeing, is $\approx 1.4''$. No absolute flux calibration was carried out. Two-dimensional calibration of the spectra was carried out with the FIGARO and MIDAS packages. Radial velocities quoted through the paper are heliocentric.

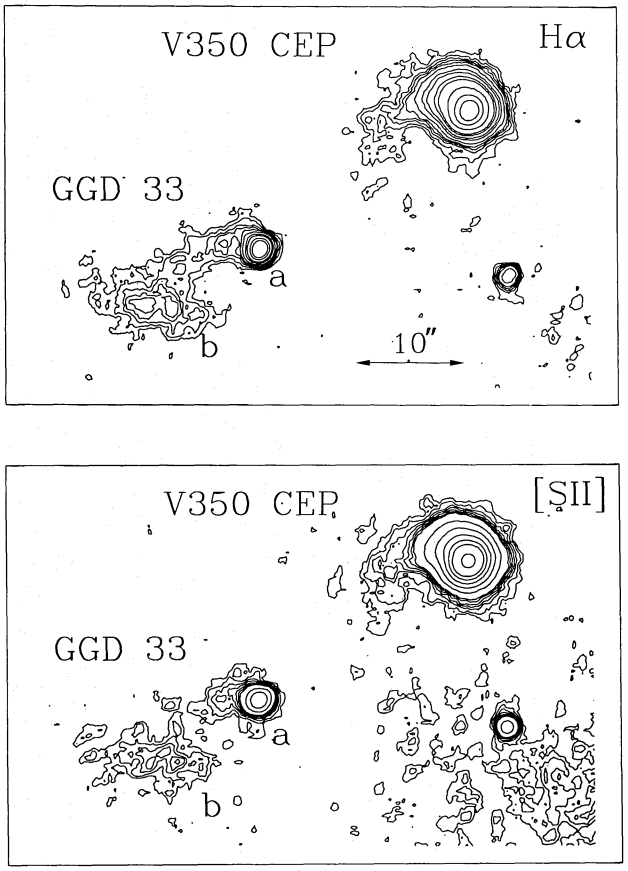

Fig. 1. Hα and [S II] isocontour plots of GGD 33 and V 350 Cep. The lowest contour is a 3σ level and 2σ level in the Hα and [S II] images, respectively; the rest is arbitrary and has been chosen to enhance the main features of the objects. North is up, east to the left

3. Results and discussion

Figure 1 shows Hα and [S II] isocontour plots of GGD 33 and V 350 Cep. Although the seeing is better than in the previous images by EGM, the morphology of GGD 33 does not present significant variations. The [S II] spike is resolved into two faint condensations: one connected to GGD 33a extending up to $\approx 2.8''$ eastwards, and one located $\approx 3.4''$ eastwards of GGD 33a. The Hα frame shows a similar structure. The stellar appearance of GGD 33a is clear. The images further show that V 350 Cep is embedded in nebulosity. The shape of the nebulosity around V 350 Cep is similar in Hα and [S II] as well as in old I images (Gómez de Castro 1989) suggesting a reflection nature.

Figure 2 presents an isophotic map, on a position-velocity (PV) plot, of the Hα region as deduced from the spectrum at PA −55°. Hα emission has been detected from GGD 33a, GGD 33b, V 350 Cep and towards the southeast of V 350 Cep. Hα radial velocities of spatially extended features are indicated in Fig. 2. Spatially extended emission is neither observed around the [S II] lines nor in the blue spectrum of V 350 Cep. GGD 33a, b have not been detected in the blue spectrum.

3.1. GGD 33

Figure 3 presents the red spectrum of GGD 33a. The Hα and [S II]6716, 6731 emission lines as well as a weak continuum are detected. The Fe II 6516 emission seems to be marginally present. The Hα emission exhibits a Beals type III P Cygni profile consisting of two emission peaks at radial velocities of ≈ -136 and $\approx +82$ km s^{-1}, separated by an absorption reversal at ≈ -80 km s^{-1}. The total velocity width (at continuum level) of the Hα emission is $\approx$ 750 km s^{-1}. The equivalent width of Hα is $\approx 110 \pm 10$ Å. The [S II] emission lines present two velocity components: a high velocity component (HVC) at ≈ -130 km s^{-1} and a low velocity component (LVC) at ≈ -16 km s^{-1} (average from both [S II] lines). From a two-component gaussian line fit to the [S II] emission features we obtain [S II]6731/6716 intensity ratios of ≈ 2.3 and ≈ 1.7, corresponding to electron densities of $\approx 1.5\ 10^5$ cm^{-3} and $\approx 3.6\ 10^3$ cm^{-3} (Pottasch 1984), in the HVC and LVC, respectively. The velocity width (FWHM) of the HVC is ≈ 34 km s^{-1} (corrected for instrumental resolution) whereas the LVC is spectrally unresolved (FWHM < 65 km s^{-1}). From GGD 33b

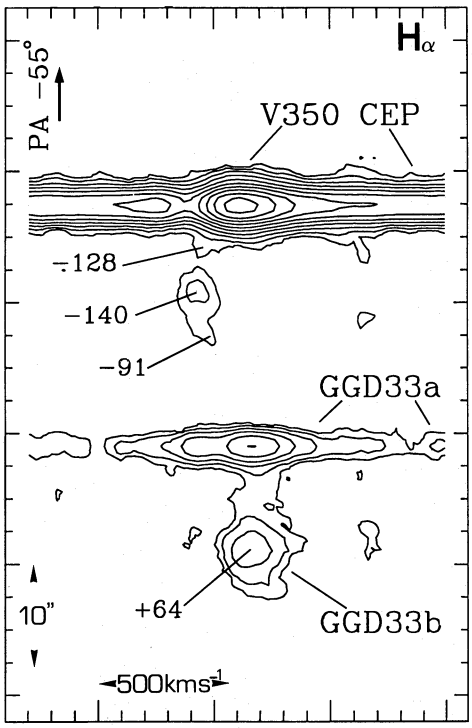

Fig. 2. Position-velocity isophotic map around the Hα emission line of V 350 Cep and GGD 33 deduced from the spectrum at PA −55° (upper left). The original data have been smoothed with a 3 × 3 box for the representation. Contours are logarithmic separated by a factor 2 in intensity. Heliocentric radial velocities (km s^{-1}) of spatially extended emission features are indicated

only Hα emission has been detected at +64 km s^{-1} (Fig. 2). The equivalent width of Hα in GGD 33b is $\approx 60 \pm 10$ Å.

GO argued that GGD 33a is a HH object with a reflection component from V 350 Cep. He based this conclusion on the emission line spectrum of GGD 33a and on the similarity between the red continua of both V 350 Cep and GGD 33a. The noticeable difference between the emission line spectrum of both objects was attributed to the finite speed of light, so that the observed spectrum of GGD 33a is actually a reflected, delayed version of the V 350 Cep one. We believe that this interpretation is, at least, controversial on the basis of the observed spectra at different epochs. If GGD 33a were reflected light from V 350 Cep, one would expect to see the rich emission line spectrum from V 350 Cep (GO, Fig. 5 and Table 1), as it is observed in reflection nebulosities associated with young stars (e.g. Mundt et al. 1985). This is not the case of GGD 33a. Except for, perhaps, line flux and/or continuum flux variations, our spectra of GGD 33a and V 350 Cep and those shown by GO and CF are essentially the same. It seems difficult to reconcile this result with a delay in the reflection due to the finite speed of light. In addition, 1) the total velocity width of the Hα emission of GGD 33a is much larger than that observed in HH objects associated with T Tauri stars, in which the total velocity width (FWZI) reaches up to ≈ 350 km s^{-1} (e.g. Böhm & Solf 1985, 1992), and 2) HH objects do not present electron densities as high as that observed in the HVC of GGD 33a (but see below).

The spectrum of GGD 33a, the Hα profile, the double-peaked [S II] emission lines, the velocity widths observed in Hα and [S II], and the red continuum are typical of T Tauri stars (Cohen & Kuhi 1979; Edwards et al. 1987; Hamann & Persson 1992). These results and the clear stellar appearance (Fig. 1) suggest that GGD 33a is a T Tauri star. In addition, the equivalent width of Hα measured in our spectrum is significatively lower than that quoted by GO, which suggests that GGD 33a exhibits the typical variability of PMS low mass stars. These results and the morphology (Fig. 1) suggest that GGD 33a is the illuminating source of the whole GGD 33 nebulosity.

The radial velocities and electron densities obtained from the [S II] lines in GGD 33a are in the range observed in other T Tauri stars. We note that the electron density of the [S II] high-velocity component of some T Tauri stars is rather high (Edwards et al. 1987) showing values up to $\geq 10^4$ cm^{-3} at small angular distances from the star (Mundt et al. 1990). The [O I]/[S II] intensity ratio ≈ 3.8 in GGD 33a

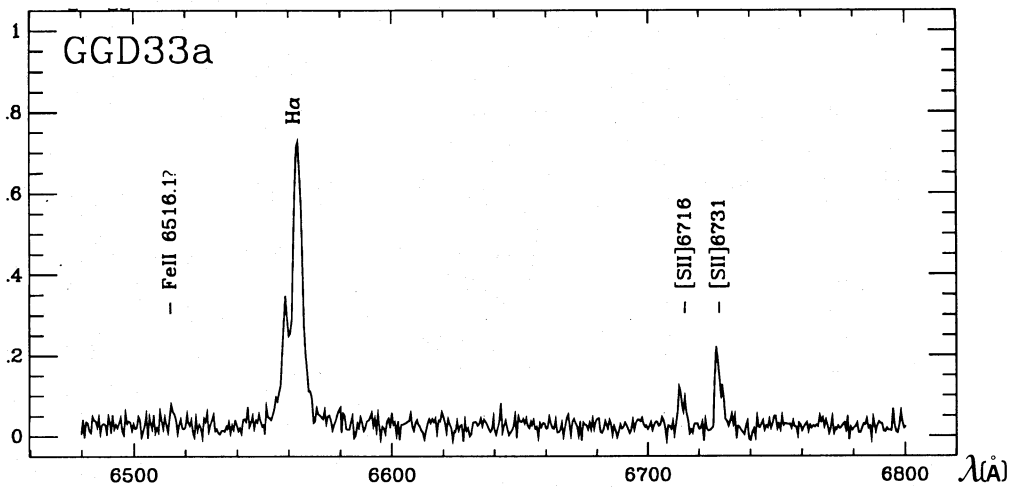

Fig. 3. Red spectrum of GGD 33a. Identified emission lines are indicated. Y-axis represents relative intensity in arbitrary units

(GO) is compatible with the electron density deduced in its [S II] HVC. This suggests that the [O II] emission may be formed, at least partially, in the same region as the HVC. Several models have been proposed in order to explain the double-peaked forbidden line profiles. Edwards et al. (1987) proposed that the lines are formed in a wind whose velocity and density depend on the latitude. Kwan & Tademaru (1988) suggested that the two components are formed in different regions, the high-velocity component arising in a jet-like outflow. Hartmann & Raymond (1989) suggested that the forbidden line emission can be explained by oblique shocks between the stellar wind and a massive circumstellar disk. The results obtained for GGD 33a seem to favor the model by Kwan & Tademaru. The large difference between the electron density in the HVC and that in the LVC suggests that the two components arise in different regions, as already pointed out in the case of other T Tauri stars (Solf 1989; Mundt et al. 1990). In addition, the velocity width (FWHM) of the HVC in GGD 33a is small compared with its radial velocity, which suggests a relatively high collimation degree for the region where the HVC arises (see Kwan & Tademaru 1988). These comments suggest that the HVC in GGD 33a may be a HH jet-like outflow observed at a very small distance from the star. If this interpretation is correct, the HVC in GGD 33a might be related to the shock-excited spike observed in [S II] images.

3.2. *V 350 Cep*

Figures 4 and 5 show the blue and red spectrum, respectively, of V 350 Cep. A high number of emission lines are observed. Proposed identifications are given in Table 1 and indicated in Figs. 4 and 5. Table 1 also gives equivalent widths for the sake of their comparison with other observations. We estimate an error of $\leq$20% in the quoted equivalent widths. It should be noted that because of the rather

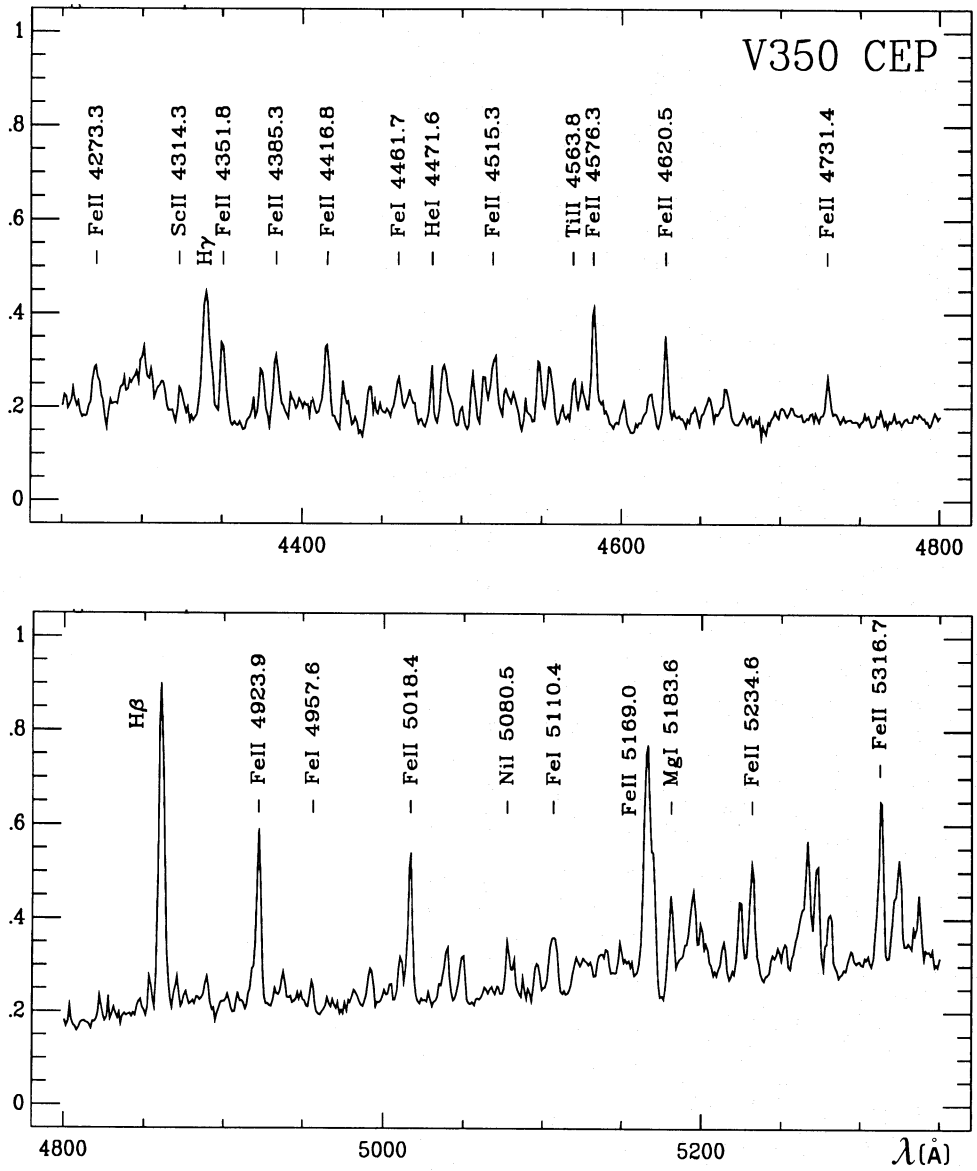

Fig. 4. Blue spectrum of V 350 Cep. Some emission lines are indicated (see Table 1). *Y*-axis as in Fig. 3

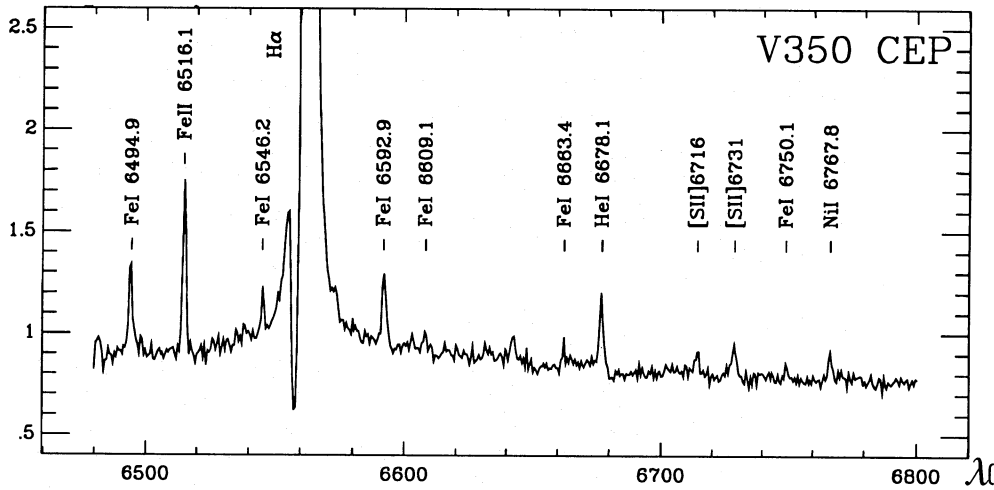

Fig. 5. Red spectrum of V 350 Cep. Some emission lines are indicated (see Table 1). Y-axis as in Fig. 3. Note that the zero intensity level is below the X-axis

moderate spectral resolution, many of the identified lines may be blends.

The following species have been detected in the spectrum of V 350 Cep: H, Fe I, Fe II, Ti I, Ti II, Sc II. He I, Cr II, Ni I, Mg I and S II. The largest number of emissions corresponds to Fe I and Fe II. Remarkably, no forbidden emission lines – excluding [S II]6716, 6731 – could be identified. The [O I]6300, 6363 emissions identified by CF and GO are outside our observed spectral range. GO identified the [N I]5199 emission in his spectrum. At this wavelength, a weak emission, blended with Fe II 5197.6 is observed in our spectrum. Comparison of the relative intensities of the lines around 5200 Å in our spectrum and in the one by GO suggests that the line detected by GO is Fe II 5197.6. Because of the low spectral resolution and blending, it is rather difficult to identify the weak emission redwards of Fe II 5197. We cannot rule out the presence of [N I]5199, but it is somewhat surprising that this is the only forbidden line in the blue spectrum and that forbidden lines of Fe I or Fe II cannot be identified. The spectrum of V 350 Cep is similar to that of AS 353A (Eislöffel et al. 1990) and that of Bretz 4 (Carballo & Eiroa 1993) in which no forbidden lines – except [S II] and/or [O I] – are observed. The absence of forbidden lines suggests the existence of high electron densities in the region of formation of the lines.

The Hα emission in V 350 Cep exhibits a Beals type III P Cygni profile, with the absorption reaching below the continuum. In Fig. 6 the Hα profile is shown in detail and heliocentric radial velocities are indicated. The weak emission at $\approx +530$ km s^{-1} is present in both the PA $-90°$ and PA $-55°$ spectra and is probably real. The equivalent width of Hα (Table 1) agrees with that measured by GO. No P Cygni profile is observed in Hβ and Hγ, although this might be due to the low spectral resolution in the blue spectrum. The [S II] emission lines present a single peak at ≈ -43 km s^{-1}. The deduced [S II]6731/6716 intensity ratio of ≈ 1.7 indicates an electron density of $\approx 3.6\,10^3$ cm^{-3}. The velocity width (FWHM) of the [S II] lines is ≈ 79 km s^{-1} (corrected for instrumental resolution). This value is rather high compared with the observed radial velocity, suggesting a poor

Table 1. Emission lines in V 350 Cep

Ion	(mult)	λ_0(Å)	W_λ(Å)
Fe II	(27)	4273.3	1.9
Fe I	(41)	4284.1	7.6
Sc II	(15)	4294.8	
Fe II	(27)	4303.7	
Sc II	(15)	4305.7	
Sc II	(15)	4314.3	—
Sc II	(15)	4325.0	1.5
Hγ		4340.5	8.4
Fe II	(27)	4351.8	4.0
Fe I	(2)	4375.3	3.0
Fe II	(27)	4385.3	4.3
Ti II	(19)	4395.0	—
Fe I	(41)	4404.8	—
Fe I	(2)	4405.0	—
Fe II	(27)	4416.8	3.3
Fe I	(2)	4427.3	1.9
Fe II	(68)	4442.3	—
Ti II	(19)	4443.8	—
Fe I	(2)	4461.7	—
He I	(14)	4471.6	1.5
Fe I	(2)	4482.2	4.5
Fe I	(2)	4489.7	0.7
Ti II	(31)	4501.3	2.3
Fe II	(38)	4508.3	—
Fe II	(37)	4515.3	—
Fe II	(38)	4541.5	—
Fe II	(38)	4549.5	5.9
Ti II	(82)	4549.6	
Ti II	(50)	4563.8	—
Fe II	(38)	4576.3	6.0
Cr II	(44)	4589.9	1.3
Ti II	(50)	4590.0	
Cr II	(44)	4618.8	4.3
Fe II	(38)	4620.5	
Fe II	(43)	4657.0	2.1
Ti II	(59)	4657.2	
Fe II	(43)	4731.4	1.9
Ti II	(92)	4805.1	—
Cr II	(30)	4824.1	0.7
Cr II	(30)	4848.2	0.7

Table 1 (continued)

Ion	(mult)	λ_0(Å)	W_λ(Å)
Hβ		4861.3	14.4
Cr II	(30)	4876.4	0.3
Fe II	(42)	4923.9	6.9
Fe I	(318)	4957.6	0.9
Fe II	(36)	4993.4	1.4
Fe II	(42)	5018.4	6.5
Ni I	(143)	5080.5	2.1
Fe I?	(66)	5098.7	1.1
Fe I	(1)	5110.4	3.1
Fe I	(37)	5166.5	10.0
Mg I	(2)	5167.3	
Fe I	(1)	5168.9	
Fe II	(42)	5169.0	
Mg I	(2)	5172.7	
Mg I	(2)	5183.6	3.1
Fe II	(49)	5197.6	—
Fe I	(36)	5216.3	—
Fe I	(37)	5227.2	1.9
Fe II	(49)	5234.6	3.2
Fe II	(48)	5234.6	
Fe I	(15)	5269.0	—
Fe II	(49)	5276.0	—
Fe II	(41)	5284.1	—
Fe II	(48)	5316.6	4.3
Fe II	(49)	5316.8	
Fe I	(49)	5325.5	3.4
Fe I	(15)	5328.0	
Fe I	(37)	5328.5	
Fe I	(37)	5341.0	1.4
Fe I	(168)	6494.9	0.9
Fe II	(40)	6516.1	1.5
Fe I	(268)	6546.2	0.3
Hα		6562.8	68.8(e)[a] −0.4(a)
Fe I	(268)	6592.9	0.8
Sc II	(19)	6604.6	0.1
Fe I	(206)	6609.1	0.2
Fe I?	(1258)	6645.2	0.3
Fe I	(111)	6663.4	0.2
He I	(46)	6678.1	0.8
[S II]	(2F)	6716.4	0.3
[S II]	(2F)	6730.8	0.5
Fe I	(111)	6750.1	0.5
Ni I	(57)	6767.8	0.3

[a] Contributions from Fe I 6546.2 and Fe I 6592.9 subtracted.

collimation degree for the region where the [S II] emission arises (see Sect. 3.1).

Figure 2 shows that blueshifted Hα emission exists towards the southeast of V 350 Cep at PA 125°. The Hα emission feature can be traced up to $\approx 14''$ from V 350 Cep. At low intensity levels, this emission feature is connected (on the PV map) to V 350 Cep. Therefore, it is reasonable to conclude that the emission is related to the star and that high velocity mass outflow emanates from

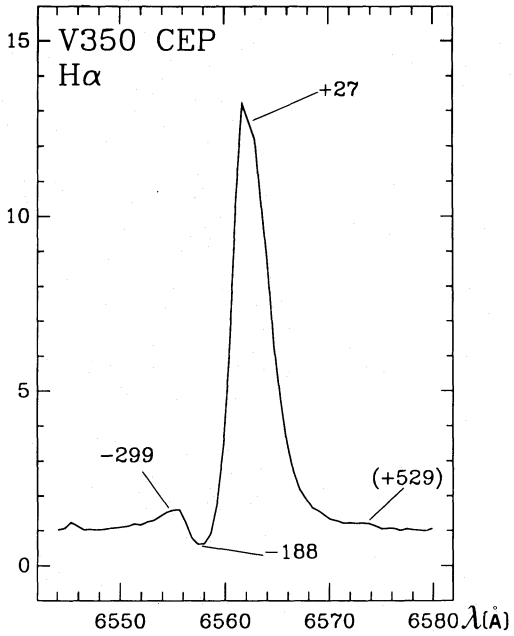

Fig. 6. Hα profile of V 350 Cep (see Fig. 5). Heliocentric radial velocities (km s^{-1}) are indicated

V 350 Cep. The radial velocity (absolute value) of the Hα emission feature increases up to a maximum value of ≈ 140 km s^{-1} at $\approx 8.5''$ from V 350 Cep and then decreases down to ≈ 90 km s^{-1} (Fig. 2). The spectrum at PA $-90°$ (not shown) does not show a similar emission feature but does present Hα emission at $\approx +25$ km s^{-1} extending up to $\approx 7''$ from the star. This emission may well be reflected light from V 350 Cep.

4. Conclusions

The main conclusions from this work can be summarized as follows:

1. GGD 33a is a variable T Tauri star and probably the illuminating source of GGD 33. Very different values of the electron density are derived for each component of the detected double-peaked blueshifted [S II] emission lines in GGD 33a. The high velocity component could be related to a HH jet-like outflow.

2. V 350 Cep is embedded in nebulosity which is mainly reflected star light. Weak blueshifted Hα emission extending from V 350 Cep suggests the existence of mass outflow from the star. The spectrum of V 350 Cep presents a large number of permitted emission lines but – except [S II] and [O I] – no forbidden emission lines have been identified.

Acknowledgements. The Calar Alto observatory is operated jointly by the Max-Planck-Institut fur Astronomie (Heidelberg) and the Spanish Comisión Nacional de Astronomía. We thank the Calar Alto staff for their help during the observations. We are grateful to F. de B. Domínguez, D. Montes and N. Cardiel for helping during the data reduction. We are grateful to an anonymous referee for

valuable comments which have improved the presentation of our results. This work is supported in part by Spanish Grants DGICYT PB87-0167, PB90-0387 and PB91-007.

References

Böhm K.-H., Solf J., 1985, ApJ 294, 533
Böhm K.-H., Solf J., 1992, AJ 104,1193
Carballo R., Eiroa C., 1993, A&A 262, 295
Cohen M., Fuller G.A., 1985, ApJ 296, 620 (CF)
Cohen M., Kuhi L.V., 1979, ApJS 41, 743
Cohen M., Schwartz R.D., 1983, ApJ 265, 877
Edwards S., Cabrit S., Strom S.E., Heger I., Strom K.M., 1987, ApJ 321, 473
Eiroa C., Gómez de Castro A.I., Miranda L.F., 1992, A& AS 92, 721 (EGM)
Eislöffel J., Solf J., Böhm K.H., 1990, A&A 237, 369
Gómez de Castro A.I., 1989, Ph.D. Thesis, Madrid
Gómez de Castro A.I., Miranda L.F., Eiroa C., 1993, A&A 267, 559
Goodrich R.W., 1986, AJ 92, 885 (GO)
Hamann F., Persson S.E., 1992, ApJS 82, 247
Hartigan P., Lada C.J., 1985, ApJS 59, 383
Hartmann L., Raymond J.C., 1989, ApJ 337, 903
Kwan J., Tademaru E., 1988, ApJ 332, L41
Magakyan T.Yu., 1983, Soviet Astron. Lett. 9, 83
Miranda L.F., Eiroa C., Gómez de Castro A.I., 1993, A&A 271, 564 (MEG)
Mundt R., Ray T.P., Bührke T., Raga A.C., Solf J., 1990, A&A 232, 37
Mundt R., Stoke J., Strom S.E., Strom K.M., Anderson E.R., 1985, ApJ 297, L41
Pottasch S.R., 1984, Planetary Nebulae. Reidel, Dordrecht
Ray T.P., Poetzel R., Solf J., Mundt R., 1990, ApJ 357, L45
Solf J., 1989, in: Reipurth B. (ed.) Low Mass Star Formation and Pre-Main-Sequence Objects. ESO Workshop, p. 399